



# Stage-Discharge Relationships of Broad Crested Weir for submerged Flow Condition Utilizing Incomplete Self-Similarity(ISS) Technique

Rawaa J.Tuama<sup>1</sup> | Mohammed S. Shamkhi<sup>1</sup>

## Affiliations

<sup>1</sup>Department of Civil Engineering, Wasit University, Kut, Iraq.

## Correspondence

Rawaa J. Tuama,  
Department of Civil Engineering, Wasit University, Kut, Iraq  
Email: [iraa.201779@gmail.com](mailto:iraa.201779@gmail.com)

## Received

13-November-2021

## Revised

28-December-2022

## Accepted

24-February-2022

Doi: [10.31185/ejuow.Vol10.Iss2.250](https://doi.org/10.31185/ejuow.Vol10.Iss2.250)

## Abstract

A broad-crested weir is one of the simplest and oldest hydraulic structures. It was used to measure flow regulate flow depth and control flood passage. Open channel flow measurement requirements are based on the experiments performed to evaluate the empirical discharge coefficients and equations. The aim of this study is to develop the stage-discharge relationships using incomplete self-similarity theory and traditional methods for calculating the discharge coefficient ( $C_{ds}$ ) and to determine which method is the most effective. All experiments were carried out in a channel with a cross-section of  $(0.5 \times 0.5)$  m and a length of 15 m. 125 experiments were carried out on 25 physical models of a broad crested weir with a rounded edge, under submerged flow conditions. The results showed, after comparing the two methods, and by calculating the mean absolute relative error (MARE) for discharges. It is equal to (4.25%) using the incomplete self-similarity theory, and it is equal to (7.05) by using the traditional method. Thus, the incomplete self-similarity formula is more accurate than the other method.

**Keywords:** Broad-crested weir, discharge coefficient, incomplete self-similarity method(ISS). mean absolute relative error (MARE)

**الخلاصة:** السد ذو القمة العريضة هو أحد أبسط وأقدم المنشآت الهيدروليكية ، فقد تم استخدامه لقياس التدفق وتنظيم عمق التدفق والتحكم في ممر الفيضان. تعتمد متطلبات قياس تدفق القناة المفتوحة على التجارب التي يتم إجراؤها لتقييم معاملات ومعادلات التصريف التجريبية. الهدف من هذه الدراسة هو تطوير علاقات Stage –discharge باستخدام نظرية التشابه الذاتي غير الكامل والطرق التقليدية لحساب معامل التفريغ ( $C_{ds}$ ) وتحديد الطريقة الأكثر فعالية. أجريت جميع التجارب في قناة ذات مقطع عرضي  $(0.5 \times 0.5)$  سم وبطول 15 م. تم إجراء 125 تجربة على 25 نموذجًا فيزيائيًا لسد عريض ذو حافة مستديرة ، في ظل ظروف تدفق المغمور. أظهرت النتائج بعد المقارنة بين الطريقتين وبحساب متوسط الخطأ النسبي المطلق (MARE) للتصاريح تساوي (4.25%) باستخدام نظرية التشابه الذاتي غير الكامل وتساوي (7.05%) عند استخدام الطريقة التقليدية بحساب معامل التصريف. وبالتالي ، فإن صيغة التشابه الذاتي غير الكامل أكثر دقة من الطريقة الأخرى.

# 1. INTRODUCTION

Weir or low head dam is a structure that spans the width of a river and changes the flow characteristics of water, usually causing a change in river level height. They're also used to control the flow of water out of the outlets of lakes, ponds, and reservoirs. Weirs come in a variety of shapes and sizes, but most allow water to flow freely over the crest before cascading down to a lower level [1 and 2]. The most common and used types of weirs are broad crested weirs. There are two types of broad-crested weirs, sharp-edged weirs, and round-edged weirs used for flow measurement in the field and laboratory. Rounding the top angle of square-edged weirs increases the discharge coefficient (Cd) and modular limit, and makes the weir less sensitive to upstream face sediment deposition, especially when the weir height is small [3]. The characteristics of the weir are also affected by the conditions of the flow, for example, the free flow or modular flow the head of the upstream is not affected by the head of the downstream, while in the submerged flow or non-modular flow the weir is submerged and the head of the upstream is affected by changes in the downstream that is when the level of the tailwater is the same height or higher than weir height[4].

The broad crested weir equation can be written in the case of free flow[5].

$$Q_f = \frac{2}{3} C_d B \sqrt{\frac{2}{3} * g H^{1.5}} \tag{1}$$

where,  $Q_f$ : actual discharge (experimental discharge) through the over the weir ( $m^3/s$ ), Cd: dimensionless discharge coefficient at free flow, B: the width of the weir in (m), H: the upstream total head above the crest (m) is equal to  $(h_1 + \frac{v^2}{2g})$ , and  $\frac{v^2}{2g}$ : Approach velocity head (m), this value may be neglected because it is very small.

In the case of submerged flow, the following equation can be obtained[6].

$$Q_s = C_{ds} h_2 B \sqrt{h_1 - h_2} * \sqrt{2 * 9.81} \tag{2}$$

Or the discharge equation for the submerge case can be calculated as follows [7]

$$Q_s = \psi Q_f \tag{3}$$

$$\psi = [1 - S^n]^m \tag{4}$$

$$S = \frac{h_2}{h_1} \tag{5}$$

where  $Q_s$  is the discharge in the case of a submerged flow [ $L^3/T$ ],  $\psi$  is the factor of submergence,  $Q_f$  The discharge is calculated using the free flow equation [ $L^3/T$ ], S is submerged ratio, n and m factors depending on the type of weir, For example, sharp-crested weir has a value of n, m equal to 1.5,0.385 respectively[7],  $h_1$  and  $h_2$  upstream and downstream head respectively as shown in Figure(1)

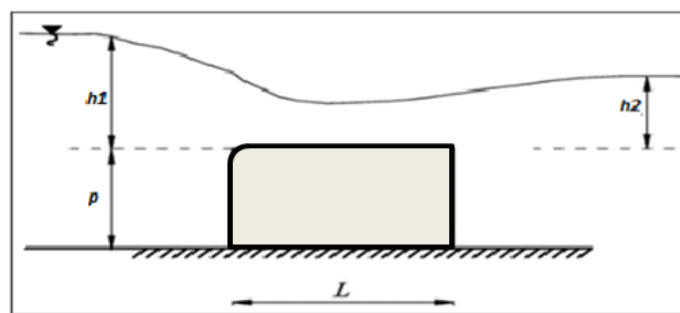


Figure 1 Broad-Crested Weir under Submerged Flow.

Stage-discharge relationships were discussed by some researchers for the free and submerged flow of various types of weirs

Azimi et al. [8] conducted an extensive experimental study to investigate the effect of submergence on a finite crest length that include (long, broad, short, sharp) crest. Various hydraulic aspects were studied such as the modular limit, water surface profiles, and discharge reduction factor. The researchers determined, through experiments, the exponent (n,m) in the submerge factor equation (4) for broad crested weir with rounded edges, which is equal to (9,1.25) respectively.

Ferro [9] The free flow of broad and sharp weir was examined and by using dimensional analysis and incomplete self-similarity theory. A head-discharge relationship was derived equally to::

$$\frac{h}{p} = a(k/p)^b \quad (6)$$

where, k is equal  $(k = \frac{Q_f^{2/3}}{B^{2/3} g})$  where (B is crest width, and g acceleration of gravity), and a, as well as b, are respectively an experimentally determined coefficient and exponent For fully-suppressed sharp-crested and broad-crested weirs, n could be equated to 1, whereas m was dependent on the geometry of the weir, according to the researcher.

Di Stefano and Ferro [10] The stage-discharge relationship was calculated using dimensional analysis and the self-similarity theory, and the outflow process of triangular in plane weirs was investigated . The stage-discharge equation can be determined using a power equation, with a coefficient and an exponent determined by the ratio of the weir's crest length to its height, as well as the sidewall angle, according to this analysis.

Hakim and Azimi. [11] The hydraulics of finite-length weirs with upstream and/or downstream slopes have been investigated under submerged flow conditions, as well as to develop practical formulas for estimating flow rate based on laboratory experiments. In addition, the location of the toe of the surface jump and surface waves downstream of the weir were investigated to see how to approach velocity affected flow patterns in submerged-flow conditions.

Dabling and Tullis [12] The objectives of this paper was to compare the behavior of a submerged piano key weir to that of a submerged labyrinth weir. The effects of tailwater submergence on the head-discharge relationships of laboratory-scale piano key weirs were explored and compared to data for labyrinth and sharp-crested linear weir submergence. The results of this research indicate that the piano key weir requires less upstream head to pass a given flow at low degrees of submergence than the labyrinth weir. This efficiency increase was just 6%, and it was reversed at greater levels of submergence.

Zachoval, et al. [13] dealt with the derivation of an equation for a broad-crested weir of a rounded edge on a theoretical basis and empirical study. The standard energy equilibrium limit equation was determined. However, the resultant equation was too complicated to be useful in practice, therefore it was approximated by a simple finite-range equation. The submerging coefficient equation was created by altering Filimonte's use of the superposition principle, and the coefficients were calculated using data from numerous authors' empirical study. The new equations compute the discharge more precisely than previous authors' equations, with an error of about 10% throughout the whole range of collected data.

Vanishree and Manjula [14] The free flow discharge equation for labyrinth weirs is unaffected by submergence up to  $S = 0.48$ .

According to the previous researches mentioned above, the application of most of the stage-discharge relationships depends on the type of weir. Most of the studies dealt with the free-flowing condition of a broad crested weir with a sharp edge. As a result, the purpose of this paper is the development of a stage- discharge relationship for a broad-crested weir with a rounded edge in the case of a submerged flow to be used for operational purposes. Where a formula is developed based on dimensional analysis and the theory of incomplete self-similarity (ISS), as well as developing a formula in the traditional method by calculating the discharge coefficient (Cds), comparing the two methods and finding the most accurate method.

## 2. MATERIALS AND METHOD

All experiments were carried out at the Iraqi Technical Institute of Kut, a hydraulic laboratory of the Middle Technical University. Dimensions of the used channel were 12 m long, 0.5 m wide, and 0.5 m deep. The flume's walls were made of glass, and the bed was from steel, illustrated in Figure 2. The outflow was measured using a

90-degree v-notch installed at the flume inlet. A moveable vertical gate was installed downstream to control the depth of the tailwater. All depth measurements were taken with two movable carriages and a 0.1 mm accuracy point gauge[1°]. The models are made of a broad-crested weir using a CNC machine to obtain the required dimensions with high accuracy. It was made of foam as shown in Figure 3. Where 125 experiments were performed on 25 models in the case of submerged flow and five discharges of 5, 10, 15, 20, and 25 l/sec were pumped for each model as mentioned in detail in Table 1. The models were placed in the middle of the channel to reduce the possible errors and to obtain accurate results. Readings were taken after a minute of waiting to ensure the water settlement.

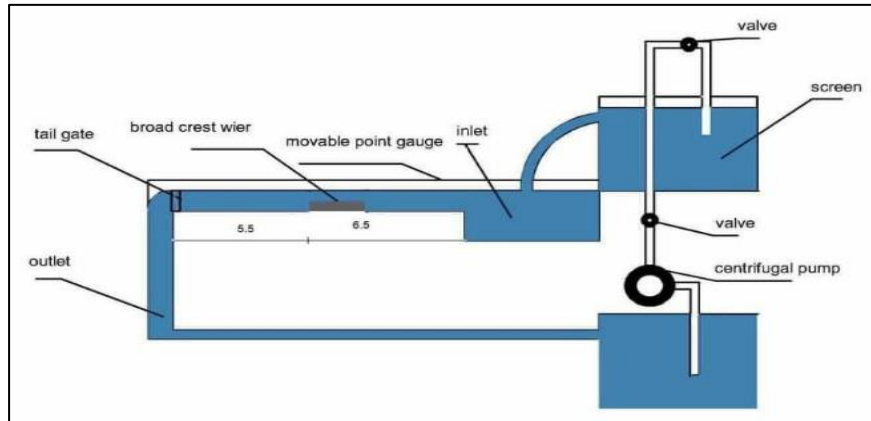


**Figure 2** A Schematic Diagram to Illustrate The Experimental Setup.



**Figure 3** Broad-Crested Weir Models Used in The Experiments.

All model dimensions conform with ASTM specifications and limitations as shown in Figure 4 [16].

- 1-  $h_1 \geq 0.06$  m
- 2-  $R \geq 0.2 h_{max}$
- 3-  $L \geq 1.75 h_{max}$ ,
- 4-  $L+R \geq 2.25 h_{max}$
- 5-  $0.05 \leq h_1/L \leq 0.57$ .
- 6-  $h/P < 1.5$
- 7-  $P \geq 0.15$  m
- 8-  $B \geq 0.3$ m or  $\geq h_1$  or  $\geq L/5$ .

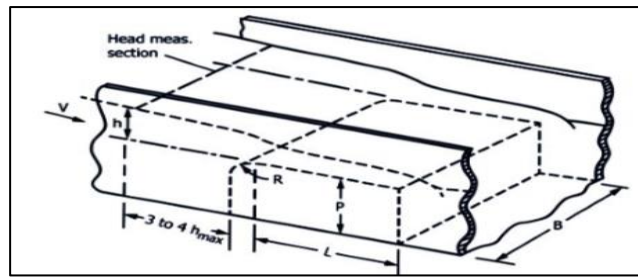


Figure 4 Specifications and Limitations of A broad-crest weir with rounded edge according to ASTM [16].

Table 1 Summary of Experimental Runs.

Runs	Height of the weir (cm)	The length of the weir (cm)	Flowrate (l/s)
1 – 5	15	30	(5, 10, 15, 20, 25)
6 – 10	15	35	(5, 10, 15, 20, 25)
11 – 15	15	40	(5, 10, 15, 20, 25)
16 – 20	15	45	(5, 10, 15, 20, 25)
21 – 25	15	50	(5, 10, 15, 20, 25)
26 – 30	20	30	(5, 10, 15, 20, 25)
31 – 35	20	35	(5, 10, 15, 20, 25)
36 – 40	20	40	(5, 10, 15, 20, 25)
41 – 45	20	45	(5, 10, 15, 20, 25)
46 – 50	20	50	(5, 10, 15, 20, 25)
51 – 55	25	30	(5, 10, 15, 20, 25)
56 – 60	25	35	(5, 10, 15, 20, 25)
61 – 65	25	40	(5, 10, 15, 20, 25)
66 – 70	25	45	(5, 10, 15, 20, 25)
71 – 75	25	50	(5, 10, 15, 20, 25)
76 – 80	30	30	(5, 10, 15, 20, 25)
81 – 85	30	35	(5, 10, 15, 20, 25)
86 – 90	30	40	(5, 10, 15, 20, 25)
91 – 95	30	45	(5, 10, 15, 20, 25)
96 – 100	30	50	(5, 10, 15, 20, 25)
101 – 105	35	30	(5, 10, 15, 20, 25)
106 – 110	35	35	(5, 10, 15, 20, 25)
111 – 115	35	40	(5, 10, 15, 20, 25)
116 – 120	35	45	(5, 10, 15, 20, 25)
121 – 125	35	50	(5, 10, 15, 20, 25)

### 3. The FIRST METHOD

#### 3.1. Dimensional analysis

The stage-discharge relationship links the main flow parameters (Figure 1) The following functional connection can be used to express it.

In dimensional analysis, the stage-discharge relationship can be expressed by the following functional relationship.

$$f(Q_s, h_1, h_2, L, B, P, g, \rho) = 0 \tag{7}$$

Using  $\rho$ ,  $g$ , and  $P$  as dimensional independent variables, the following dimensionless variables were found.

$$\pi_1 = \rho^{a1} g^{b1} P^{c1} Q_s$$

$$\pi_2 = \rho^{a2} g^{b2} P^{c2} h_1$$

$$\pi_3 = \rho^{a3} g^{b3} P^{c3} L$$

$$\pi_4 = \rho^{a4} g^{b4} P^{c4} B$$

$$\pi_5 = \rho^{a5} g^{b5} P^{c5} h_2$$

Expressing these in dimension terms the following is obtained.

$$\pi_1 = \rho^{a1} g^{b1} P^{c1} Q_s$$

$$\pi_1 = \frac{Q_s}{p^{2.5} \sqrt{g}}$$

$$\pi_2 = \rho^{a2} g^{b2} P^{c2} h_1$$

$$\pi_2 = \frac{h_1}{p}$$

$$\pi_3 = \rho^{a3} g^{b3} P^{c3} L$$

$$\pi_3 = \frac{L}{p}$$

$$\pi_4 = \rho^{a4} g^{b4} P^{c4} B$$

$$\pi_4 = \frac{B}{p}$$

$$\pi_5 = \rho^{a5} g^{b5} P^{c5} h_2$$

$$\pi_5 = h_2/p$$

By combining the groups  $\pi_1$  and  $\pi_4$ , the following is obtained.

$$\pi_{(1,4)} = \frac{\pi_1}{\pi_4} = \frac{p}{h_1} \frac{h_2}{p} = \frac{h_2}{h_1}$$

The following relationships can also be obtained by combining.

$$\pi_{(3,4)} = \frac{\pi_3}{\pi_4} = \frac{Q_s^{2/3}}{g^{1/2} p^{5/2}} \frac{p^{2/3}}{B^{2/3}} = \psi \left( \frac{K_s}{p} \right)^{3/2}$$

$\psi$  = reduction factor calculated from the following equation.

$$K_s = \frac{Q^{2/3}}{g^{1/3} B^{2/3}}$$

Eq. 7 can be expressed in a dimensionless form as follows:

$$\pi_{3,4} = F(\pi_1, \pi_2, \pi_3, \pi_5) \tag{8}$$

The functional relationship in Eq. 8 can be rewritten in the following form.

$$\psi (k_s/p)^{1.5} = f\left(\frac{h_2}{h_1}, \frac{h_1}{p}, \frac{L}{p}\right) \tag{9}$$

### 3.2. Incomplete self-similarity (ISS) theory

When the functional relationship  $\pi_1 = f(\pi_2, \pi_3, \dots, \pi_n)$  expressing a physical phenomenon is independent of  $n$ , the phenomenon is considered self-similar in the dimensionless group  $\pi_n$ . The behavior of (f) is investigated for  $\pi_n \rightarrow 0$  or  $\pi_n \rightarrow \infty$ . A problem's self-similarity solutions are investigated for boundary conditions, i.e., the behavior is studied for  $\pi_n \rightarrow 0$  or  $\pi_n \rightarrow \infty$ . The phenomenon is expressed by the functional relationship  $\pi_1 = f(\pi_2, \pi_3, \dots, \pi_{n-1})$ .

where 1 represents the functional symbol and self-similarity is referred to a complete self-similarity (CSS) in a given n dimensionless group.

When the function approaches a finite limit and it is not zero. The following functional relationship expresses the phenomenon:  $\pi_n = \pi_n^\epsilon f(\pi_2, \pi_3, \dots, \pi_{n-1})$ . Incomplete self-similarity (ISS) is the word used in the parameter  $\pi_n$  to describe this situation [ $1^V$  and  $1^\wedge$ ].

The mathematical shape of the functional relationship Eq. 8 can be deduced using the ISS method because

$\frac{h_1}{p} \rightarrow 0$  Then,  $\psi\left(\frac{k_s}{p}\right)^{1.5} \rightarrow 0$  and when  $\frac{h_1}{p} \rightarrow \infty$  then

$\psi\left(\frac{k_s}{p}\right)^{1.5} \rightarrow \infty$  to use this method the ISS occurs. Therefore, Eq. 9 becomes

$$\psi\left(\frac{k_s}{p}\right)^{1.5} = c \left(\frac{h}{p}\right)^r \left[\frac{h_2}{h_1}\right]^t \quad \text{According to } (L/p) \quad (10)$$

c, t and r are numerical constants calculated experimentally.

### 3.3 Development of a stage-discharge relationship for the submerged flow case

To complete the derivation of the special equation for the submerged flow condition of the broad-crested weir with a rounded edge, the experimental results for the case of the submerged flow are collected. Based on Eq. 9, a relationship between  $h/p$  and  $\Psi(k_s/p)^{1.5}$  must be plotted according to  $L/p$  as shown in Figure 5. From Figure (5), the following Eq. 10 can be obtained.

$$\psi\left(\frac{k_s}{p}\right)^{1.5} = 0.5154 \left(\frac{h}{p}\right)^{1.5417} \quad (11)$$

To show the possibility of the ISS, plot a relationship between submerge ratio  $\frac{h_2}{h_1}$  with  $cs^*$  according to  $L/p$ . As shown in Figure 6, where  $cs^*$  can be determined by the following formula.

$$cs^* = \frac{\psi\left(\frac{k_s}{p}\right)^{1.5}}{\left(\frac{h}{p}\right)^{1.5417}}$$

Thus, the following equation from Figure 6.

$$cs^* = c \left(\frac{h_2}{h_1}\right)^t \quad (12)$$

The values of c and t illustrated in the table (2).

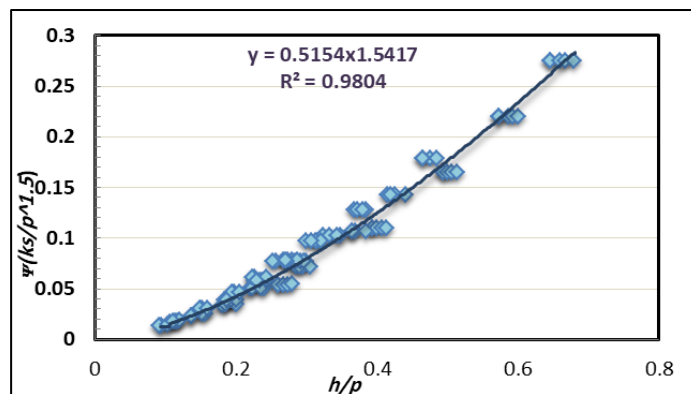


Figure 5 Relationship between  $\Psi(k_s/p)^{1.5}$  and The Ratio  $(h_1/p)$ .

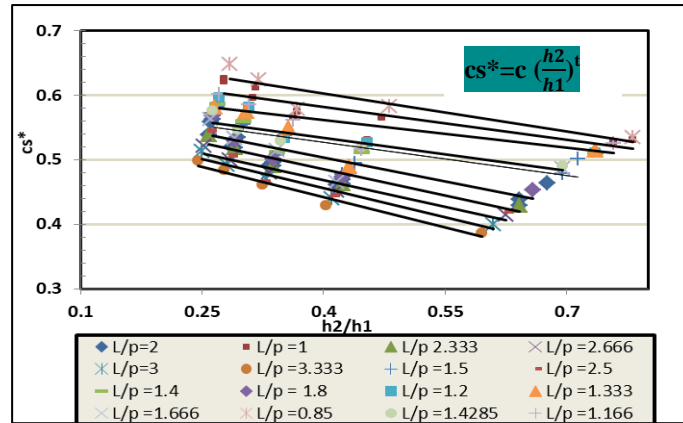


Figure 6 Relationship between  $(h_2/h_1)$  with  $cs^*$  According to  $L/p$ .

Table 2 The Values of Constants  $c$  and  $t$  from Figure 6.

$L/p$	$C$	$t$	$L/p$	$C$	$t$
2	0.3924	0.23	1.4	0.4791	0.118
1	0.4989	0.156	1.8	0.4021	0.229
2.333	0.3793	0.249	1.2	0.4778	0.15
2.666	0.3654	0.252	1.333	0.4754	0.137
3	0.3466	0.277	1.666	0.4434	0.146
3.333	0.3317	0.291	0.85	0.5082	0.174
1.5	0.4478	0.165	1.4285	0.4609	0.149
2.5	0.3589	0.273	1.166	0.4904	0.139

Figure (7) depicts the relationship between  $c$  and  $L/p$  in order to obtain Eq. 13.

$$c = 0.5097 (L/p)^{-0.348} \tag{13}$$

Furthermore, the relationship between  $t$  and  $L/p$  is shown in Figure 8 to get the following equation.

$$t = 0.1358 (L/p)^{0.6174} \tag{14}$$

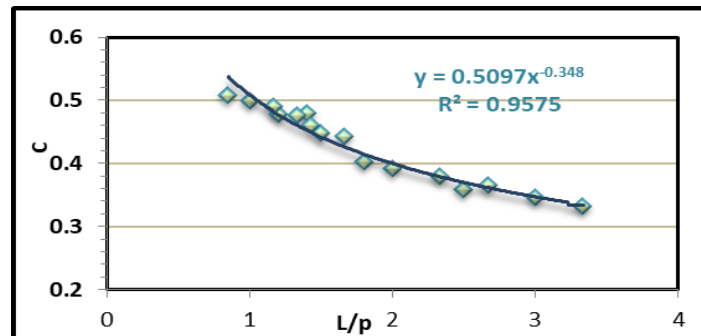


Figure 7 Relationship between The Values of  $(c)$  and relative  $(L/p)$ .

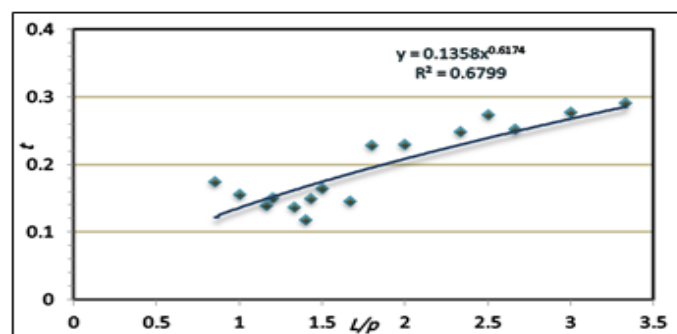


Figure 8 Relationship between The Values of  $(t_1)$  and  $(L/p)$ .

By substituting Eqs. 12, 13, and 14 in Eq. 10, the general equation for submerged flow for a broad-crested weir depending on L/p is as follows

$$\left[ \psi \left( \frac{k_s}{p} \right)^{1.5} = (0.263) \left( \frac{h}{p} \right)^{1.5417} \left[ \left( \frac{L}{p} \right)^{-0.348} \left( \frac{h_2}{h_1} \right)^{(0.1538)} \left( \frac{L}{p} \right)^{0.3174} \right] \right] \tag{15}$$

## 4. THE SECOND METHOD

### 4.1. Determination of discharge coefficient for submerged flow

The parameters can be expressed in the functional relationship:

$$C_{ds} = (\rho, \mu, h_2, h_1, g) \tag{16}$$

Using Buckingham's theorem for connection  $C_{ds}$  with ratio  $\left( \frac{h_2}{h_1} \right)$  may be expressed as:

$$C_{ds} = f \left( \frac{h_2}{h_1} \right) \tag{17}$$

As for the  $C_{ds}$  calculation for the submerged flow case, it is calculated from the following equation [22].

$$C_{ds} = \frac{Q_s}{h_2 B \sqrt{h_1 - h_2} \sqrt{2 * 9.81}} \tag{18}$$

According to equation (18), the relationship between the discharge coefficient ( $C_{ds}$ ) and the submerged ratio  $\left( \frac{h_2}{h_1} \right)$  is plotted as shown in Figure 9, which shows that the relationship is inverse. As the submerged ratio increases, the value of the discharge coefficient ( $C_{ds}$ ) decreases according to Eq. 20.

$$C_{ds} = 0.5925 \left( \frac{h_2}{h_1} \right)^{-0.737} \tag{19}$$

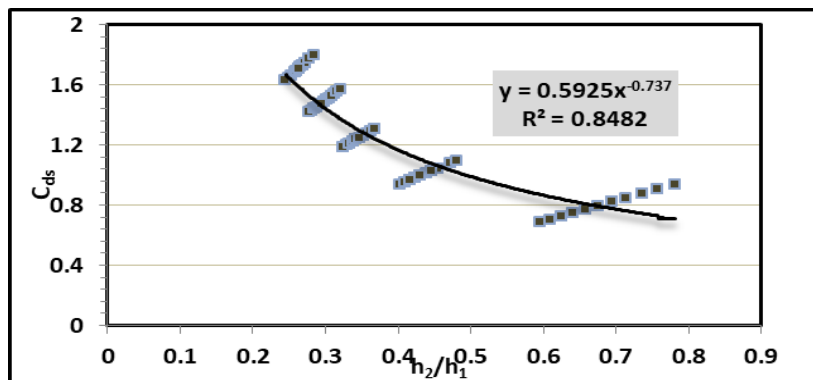


Figure 9 The Relationship between submerge ratio ( $h_2/h_1$ ) and discharge coefficient  $C_{ds}$ .

## 5. VERIFICATION OF THE STAGE-DISCHARGE FORMULA FOR THE SUBMERGED FLOW

It is necessary to verify the two Eqs. 15 and 19 by calculating the discharge for each of them ( $Q_{est}$ ). This can be done by substituting the experimental results of the experiments that did not use in its derivation when ( $L/p= 1.6$ ,  $L/p= 2.25$ ,  $L/p= 1.14$ , and  $L/p= 1.28$ ) and comparing it with the experimental discharge ( $Q_m$ ). It is observed that the determination of coefficient ( $R^2$ ) is high between  $Q_m$  with  $Q_{est}$  (eq. 15 and eq. 19) as shown in Figure 10. But MARE% differs, and it is equal to 4.5 and 7.05 by equations (14 and 18), respectively. Thus, Eq. 15 is more accurate than Eq. 19.

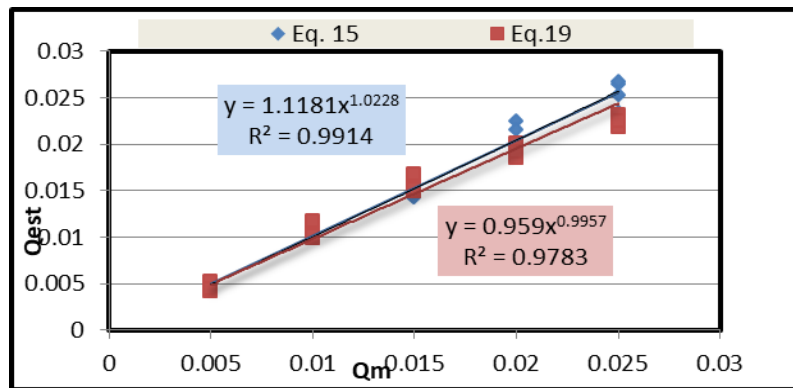


Figure 10 Relationship between discharge experimental ( $Q_m$ ) and discharge calculated by (eqs.15,19) ( $Q_{est}$ )

## 6. CONCLUSION

In this study, the stage-discharge relationships of the submerged flow condition of a broad-crested weir with a rounded edge were investigated. In the case of changing the dimensions of the weir, which included many scenarios, the most important results were included in this study.

- 1- Develop formulas for the stage-discharge for the case of submerging flow based on the dimensional analysis and incomplete self-similarity (ISS).
- 2- Develop formulas to calculate the discharge coefficient based on dimensional analysis based on the dimensionless coefficient ( $h_2/h_1$ ), which represents the submerge ratio. The values of the discharge coefficient range from (0.45 to 1.85).
- 3- the two equations (15 and 19) are verified after calculating the discharge for each of the two formulas and comparing them with the experimental discharges. It can be concluded when calculating the mean that the derived equation based on the incomplete self-similarity theory (Eq.15) is more accurate than the other (Eq.19), where the mean absolute relative error is (4.25, 5.0%) respectively.

The experimental investigation confirmed the applicability of the theoretical relationships extracted from the discharge stage (15 and 19) calibrated with specific measurements.

### SYMBOLIZATIONS:

- $g$ : the acceleration due to gravity.
- $\mu$ : dynamic viscosity.
- $P$ : The height of the weir.
- $L$ : The length of the weir.
- $B$ : channel width and width of the broad crest weir.
- $y_1$ : the water depth upstream.
- $h_1$ : Upstream head.
- $h_2$ : downstream head.
- $h_1$ : the head over the weir (upstream head).
- $k_s$ : critical depth.
- $C_{ds}$ : coefficient of discharge submerge flow.
- $Re$ : Reynolds number.
- $We$ : Weber number.
- $c, t, r$ : numerical constant.
- $(Q_m)$ : discharge experimental.
- $(Q_{est})$ : discharge calculated by (eqs.15,19).
- $\psi$ : reduction factor

## REFERENCES

1. Fritz, H. M., and Hager, W. H. (1998). Hydraulics of embankment weirs. *Journal of Hydraulic Engineering*, **124**(9), 963-971.
2. Herschy, R. W. (1995). Streamflow measurement. Second Edition, E and FN Spon, an Imprint of Chapman and Haii, London, UK.
3. Ramamurthy, A. S., Tim, U. S., and Rao, M. V. J. (1988). Characteristics of square-edged and round-nosed broad-crested weirs. *Journal of Irrigation and Drainage Engineering*, **114**(1), 61-73.
4. Wu, S., and Rajaratnam, N. (1996). Submerged flow regimes of rectangular sharp-crested weirs. *Journal of Hydraulic Engineering*, **122**(7), 412-414.
5. Bos, M. G. (1989). Discharge measurement structures. Third Revised Edition, *International Institute for land Reclamation and Improvement /ILRI*.
6. Nikolov, N. A., Minkov, I. N., Dimitrov, D. K., Mincheva, S. K., and Mirchev, M. A. (1978). Hydraulic calculation of a submerged broad-crested weir. *Hydrotechnical Construction*, **12**(6), 631-634
7. Villemonte, J. R. (1947). Submerged weir discharge studies. *Engineering News Record*, **139**(26), 54-56.
8. Azimi, A. H., Rajaratnam, N., and Zhu, D. Z. (2014). Submerged flows over rectangular weirs of finite crest length. *Journal of Irrigation and Drainage Engineering*, **140**(5), 06014001.
9. Ferro, V. (2011). A new solution of the stage-discharge relationship for sharp-crested and broad weir. *Italia Forestale e Montana*, **66**(2), 127-139.
10. Di Stefano, C., and Ferro, V. (2013). A new approach for deducing the stage-discharge relationship of triangular in plan sharp-crested weirs. *Flow Measurement and Instrumentation*, **32**, 71-75.
11. Hakim, S. S., & Azimi, A. H. (2017). Hydraulics of submerged triangular weirs and weirs of finite-crest length with upstream and downstream ramps. *Journal of Irrigation and Drainage Engineering*, **143**(8), 06017008.
12. Dabling, M. R., and Tullis, B. P. (2012). Piano key weir submergence in channel applications. *Journal of Hydraulic Engineering*, **138**(7), 661-666.
13. Zachoal, Z., Major, J., Roušar, L., Rumann, J., Šulc, J., and Jandora, J. (2019). Submergence coefficient of full-width sharp-edged broad-crested rectangular weirs. *Journal of Hydrology and Hydromechanics*, **67**(4), 329-338.
14. Vanishree, B. R., and Manjula, R. (2018). Analysis of various parameters affecting weir design and fabrication of weirs: An overview. *MATEC Web of Conferences*, 144, 01006.
15. Shamkhi, M.; Hafudh, A.; Qais, H.; and Amer, R. (2019). Froude number data analysis and its implications on local scour. 12th International Conference on Developments in eSystems Engineering (DeSE). Kazan, Russia, 315-320.
16. ASTM International Designation. (2014). Standard guide for selection of weirs and flumes for open-channel measurement of water. United States.
17. Barenblatt, G. I. (1979). Similarity, self-similarity and intermediate asymptotics. Consultants Bureau, New York.
18. Barenblatt, G. I. (1987). Dimensional analysis. Gordon and Breach, Science Publishers, Amsterdam, Netherlands.